From phonons to the thermal properties of complex thermoelectric crystals: The case of type-I clathrates

Stéphane Pailhes, Valentina M. Giordano, Shelby R Turner, Pierre-François Lory, Christophe Candolfi, Marc de Boissieu, Holger Euchner

Results in Physics 49 (2023) 106487

Contents lists available at ScienceDirect

Results in Physics

journal homepage: www.elsevier.com/locate/rinp

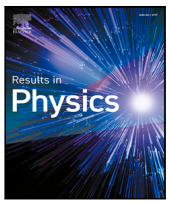

From phonons to the thermal properties of complex thermoelectric crystals: The case of type-I clathrates

S. Pailhès [a,*,1], V.M. Giordano [a], S.R. Turner [a], P.-F. Lory [b], C. Candolfi [c], M. de Boissieu [b], H. Euchner [d,*]

[a] Institute of Light and Matter, UMR5306 Université Lyon 1-CNRS, Université de Lyon., Campus LyonTech - La Doua, 69622, Villeurbanne, France
[b] SIMAP, UJF, CNRS, INP Grenoble, 38402, St Martin d'Hères, France
[c] Institut Jean Lamour, UMR 7198 CNRS – Universitè de Lorraine, Campus ARTEM, 2 allée André Guinier, 50840, 54011, Nancy, France
[d] Institute of Physical and Theoretical Chemistry, Emmy-Noether Group Specsy, University of Tübingen, Auf der Morgenstelle 15, 72076, Tübingen, Germany

ARTICLE INFO

Keywords:
Crystal complexity
Phonons
Lattice thermal conductivity
Heat capacity
Thermoelectricity
Clathrates

ABSTRACT

Exploiting the structural complexity of crystals at the scale of their unit cell is a well-established strategy in the search for efficient materials for energy conversion, which aims at disentangling and separately engineering heat and charge transport. This route has resulted in the discovery of clathrates with exceptionally low lattice thermal conductivity but essentially unaffected and tunable electronic properties. Although their thermal conductivity behaves similarly to the one of glasses, its origin is fundamentally different. Indeed, phonons with long lifetime were observed over the whole Brillouin zone, thus excluding an interpretation in terms of a reduced mean free path. However, the energy–momentum phase space which contains these heat carrying phonons is capped by a dense spectrum of diffusive modes. The thermal properties of clathrates can therefore be split in two parts: a narrow low energy regime that contains propagative modes which dominate the thermal transport, and a broad high energy range consisting of diffusive modes that dominate the heat capacity. Based on this understanding, a simple phenomenological model, based on a basic description in terms of Debye and Einstein modes, is derived that allows for a meaningful interpretation of experimental data, by providing a connection to the underlying microscopic origin. Finally, the criteria for determining the minimum lattice thermal conductivity are redefined and strategies for decreasing the lattice conductivity are proposed.

Introduction

Designing the phonon spectrum of energy-efficient semiconductors, *i.e.* controlling the channels through which heat is conveyed or photo-electrons release their energy, is an important challenge, common to many applications such as thermoelectric [1] and photovoltaic [2,3] conversion, phase change memories [4], and battery electrodes [5,6]. Structural complexity, which can easily result in unit cells in the nanometer range that contain a large number of atoms of various types, is known to be an efficient way for designing thermal properties and the underlying phonon spectra. In the search for low lattice thermal conductivity (κ_L) in the field of thermoelectricity, one of the main strategies is the use of complexity at multiple length scales, from structural complexity within the crystal unit cell, to disorder, short range order, and nanostructuring [7–9]. Crystals with a high structural complexity and chemical bonding inhomogeneity [10], such as tetrahedrites [11], skutterudites [12] or type-I clathrates [13], often have a very low and almost temperature independent κ_L of ~0.5–2 W m^{-1} K^{-1} in the 50–500 K range. In this article, we will focus on the case of type-I inorganic clathrates where a large amount of experimental and theoretical works has contributed to a detailed understanding of the microscopic origin of their anomalous thermal properties. They represent a large family of so-called cage compounds, which are built up by a three-dimensional arrangement of polyhedra of typically group 14 elements in which mostly alkaline-earth guest atoms reside as exemplified in Fig. 1(a) for a Ba-encapsulating Ge-based type-I clathrate. Type-I clathrates are typically described in a cubic space group with a lattice parameter of about 1 nanometer. While the chemistry of these guest-host structures allows to vary their electrical properties going from semiconductors, to metals or even superconductors, their probably most fascinating property, associated with their structural complexity, is their very low and smoothly temperature dependent lattice thermal conductivity [7,8,10]. As illustrated in Fig. 1(b), the lattice thermal

* Corresponding authors.
E-mail addresses: stephane.pailhes@univ-lyon1.fr (S. Pailhès), holger.euchner@uni-tuebingen.de (H. Euchner).

[1] S. Pailhès acknowledges support from the French National Research Agency (ANR-13-PRGE-0004 and ANR-21-CE08-0045).

https://doi.org/10.1016/j.rinp.2023.106487
Received 7 December 2022; Received in revised form 21 April 2023; Accepted 23 April 2023
Available online 27 April 2023

conductivity of a type-I Ge-based clathrate is typically two orders of magnitude lower than that of pure Ge at room temperature and this difference increases upon cooling. On the other hand, phonon measurements by means of inelastic neutron/X-ray scattering (INS/IXS) have revealed the existence of long-living acoustic phonons in clathrates, thus questioning the origin of their low lattice thermal conductivity [14–17]. However, this is not specific to clathrates and is found in many crystalline materials with a complex crystallographic structure such as in the thermoelectric skutterudites or tetrahedrites [11,18], in photovoltaic hybrid perovskites [2], or in quasicrystals [19,20]. The current understanding is that the heat conduction is mostly conveyed by well-defined acoustic phonons, which exist only in a limited range of the energy and momentum phase space, capped by a continuum of nondispersive optical phonon bands [15–17,21–23]. This can be seen in Fig. 1(b–c) where phonon spectra in pure Germanium and in a Ge based type-I clathrate are compared. The large number of atoms in the clathrate unit cell leads to a large number of vibrational states which form a dense continuum of optical branches, thus limiting the phase space available for the acoustic phonons and thus efficiently reducing the heat conduction. The onset of this continuum defines the upper limit in energy of the acoustic regime such that it has been associated with a low-pass filter for acoustic phonons [17] or a modified Debye energy [21,24]. Its position in energy controls the room temperature value of the lattice thermal conductivity [24] while its temperature dependence was found to be responsible for the smooth variation of the lattice thermal conductivity with temperature [14,25]. On the other hand, the onset of the optical continuum can be changed by varying the chemical composition [15] or the structural topology [26], *i.e.* by modification of the cage structure.

In this work, starting from a microscopic understanding of the lattice dynamics in type-I clathrates [14–17,22,27,28], simple phenomenological models – based on a description in terms of Debye and Einstein modes – for thermal properties such as isochoric heat capacity (C_v) and lattice thermal conductivity (κ_L) are derived. While first principle approaches are in principle capable to give access to these quantities, the proposed models can easily be applied to fit experimental data and, despite their simplicity, allow to extract the relevant microscopic parameters of the underlying phonon spectrum. Apart from deriving physically meaningful models for the case of type–I clathrates as well as other structurally complex materials, this paper aims at highlighting the potential misinterpretations of unsuited fitting approaches. Finally, an expression for the minimum of the lattice thermal conductivity in type-I clathrates is given and the microscopic parameters which enable reaching this limit are identified, guiding future efforts to further decrease the lattice thermal conductivity and thus optimize the thermoelectric efficiency.

A simplified description of the phonon spectrum

As sketched for the case of a Ge-based type-I clathrate (see Fig. 2), the phonon spectrum of structurally complex crystals can typically be divided in two main parts in energy on both sides of the energy labeled $\hbar\omega_{op}$: the acoustic part, which contains well defined propagative Debye like acoustic modes involving coherent collective motions of guest and host atoms, and the optical part (red area), which contains a distribution of dispersion-less Einstein like optical phonons. The energies of the optical modes spread up to a high energy cut-off labeled $\hbar\omega_{max}$. This partition of the phonon spectrum between a Debye and a Einstein regime results from the large number of atoms within the crystal unit cell while the values of the energies $\hbar\omega_{op}$ and $\hbar\omega_{max}$, the sound velocities of the acoustic modes and the distribution of modes within the Einstein part depend on the chemistry and the topology of the unit cell.

It has been measured by Neutron Resonant Spin Echo (NRSE) spectroscopy that the lifetime of an acoustic phonon in a type-I clathrate, located in the middle of the acoustic branch (with an energy of 2 meV),

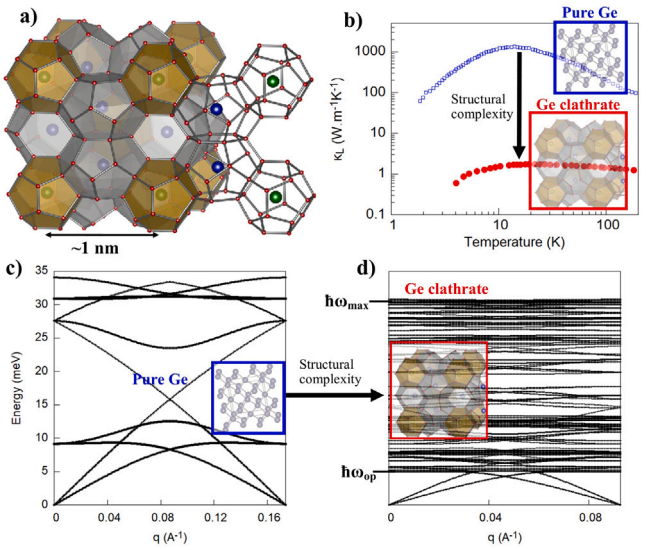

Fig. 1. Impact of the structural complexity on the lattice dynamics. (a) The type-I clathrate crystal unit cell (cubic, lattice parameter of about 1 nm), here the case of $Ba_{7.81}Ge_{40.67}Au_{5.33}$(BAG), contains tetrahedrally coordinated host atoms of group 14 elements (Si,Ge,Sn) arranged in a 3D covalent framework of face-sharing dodecahedra (in gold color) and tetrakaidecahedra (in silver color) encapsulating guest cations. (b) Temperature dependences of the lattice thermal conductivity measured in pure Ge (blue open squares) [29] and in BAG (red filled circles) [15,30]. (b)–(c) Phonon dispersion curves for pure Ge and BAG as obtained from DFT calculations using the meta-GGA functional SCAN [27]. (For interpretation of the references to color in this figure legend, the reader is referred to the web version of this article.)

amounts to about 30 ps. This results in a mean free path of about 30 nm at room temperature, thus being one order of magnitude larger than the size of the unit cell which confirms the propagative nature of these modes [15]. On the other hand, optical phonons with energies higher than $\hbar\omega_{op}$ are almost dispersionless with very low group velocity, often only involving vibrations of some specific atoms in the unit cell. As they are numerous and with high energies, they dominate the heat capacity but contribute much less efficiently to the heat transport than the acoustic modes.

In this perspective, a simple description of the lattice isochoric heat capacity (C_v) and thermal conductivity (κ) can be obtained as a sum of a Debye (D) and an Einstein (E) contribution directly related to the acoustic and optic parts, respectively:

$$C_v = C_v^D + C_v^E$$
$$\kappa = \kappa_D + \kappa_E \quad (1)$$

The energy $\hbar\omega_{op}$ defines the transition between the Debye ($\hbar\omega < \hbar\omega_{op}$) and the Einstein ($\hbar\omega \geq \hbar\omega_{op}$) regimes. The cut-off energy $\hbar\omega_{max}$ is the maximal optical phonon energy. These energies can be easily measured by standard inelastic spectroscopy techniques (Raman, IXS or INS) on polycrystalline samples. Furthermore, it will be shown below that, with the appropriate model, they can also be extracted precisely from heat capacity measurements.

The heat capacity of complex crystals

In the following, we start by reviewing the model commonly used to fit heat capacities in type-I clatrates – and other cage based and complex materials – which will be referred to as “classical Debye model” below. First, it will be shown that the microscopic picture on which this model relies is not coherent with the phonon spectrum of a type-I clathrate. After discussing the misconceptions of this approach, an alternative and simple macroscopic model, “the capped Debye model”, is proposed.

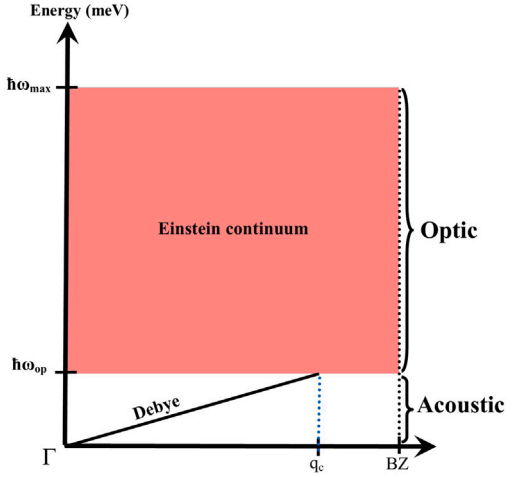

Fig. 2. Schematic representation of the phonon spectrum in a structurally complex crystal. The phonon spectrum represented in the first Brillouin zone (BZ) can be split in two spectral ranges at both sides of a threshold energy called $\hbar\omega_{op}$: the acoustic and the optic regime. The acoustic phonons describe a Debye-like linear branch, $\hbar\omega = v_s q$ with v_s the average sound velocity, which is stopped at (q_c, $\hbar\omega_{op}$) when it hits the low energy edge of a dense continuum of dispersion-less optical Einstein phonons which have energies distributed from $\hbar\omega_{op}$ to a high energy cut-off at $\hbar\omega_{max}$. (For interpretation of the references to color in this figure legend, the reader is referred to the web version of this article.)

The classical Debye model: interpretation and failure

For a long time, the crystal structure of type-I clathrates has been viewed as host network filled by loosely bound guest atoms, so-called "*rattlers*", which were assumed to be isolated from each other. To model the lattice dynamics of such materials in a simple and intuitive approach, the host network was considered as a stiff Debye solid, while the network of rattlers was describes as a system of independent Einstein oscillators. A well known representation of the corresponding microscopic phonon spectrum has been illustrated in [31] (see Figure 4 of that paper). In this context, the rattling vibrations couple with the host acoustic phonons only in a confined region of the energy and momentum phase space, when their energies become comparable, leading to a so-called "*avoided crossing*" between the host and guest phonon branches. In coherence with this microscopic picture, the Debye and the Einstein contributions to heat capacity and lattice thermal conductivity, as decomposed in Eq. (1), were attributed to host and guest networks respectively [32]. The earlier experimental reports of the lattice thermal properties in crystalline clathrates of type-I like $(Eu,Sr,Ba)_8Ga_{16}Ge_{30}$ [33–35], $Ba_8Ga_{16}X_{30}$ (X = Ge,Sn) [35,36], $Sr_8Ga_{16}Si_{30-x}Ge_x$ [37], $Ba_8Ga_{16}Sn_{30}$ [38,39], $Ba_8Zn_{7.7}Ge_{38.3}$ [40] and $Ba_8Ni_xGe_{46-x}$ (x = 3, 4, 6) [41] resulted in the derivation of this heuristic model. Due to its apparent success, this model has become very popular for the analysis and comparison of thermal properties in type-I clathrates. Later, the application of this model has even been extended to other cage-based materials, such as skutterudites [42] and pyrochlores [43].

By applying this model to type-I clathrates, the Debye component is assumed to describe the lattice vibrations of $n_H = 46$ host atoms per unit cell. In a 3D solid, each of these atoms has three independent vibrational degrees of freedom. Consequently, the number of vibrational modes is given by $3n_H = 138$. In the basic Debye approach, these modes define a linear and isotropic dispersion following $\hbar\omega = v_s|\mathbf{q}|$, where v_s is the average sound velocity, as calculated from the slope of the two TA and the LA phonon dispersions: $\frac{3}{v_s^3} = \frac{2}{v_{TA}^3} + \frac{1}{v_{LA}^3}$. It has to be noted that optical phonons are not accounted for in the Debye model, as it is originally based on a mono-atomic cubic lattice. The maximum energy of this linear dispersion, called the Debye energy $\hbar\omega_D$ (with the associated Debye temperature $k_B\Theta_D$), is then simply determined by the total number of host phonon modes, *i.e.*, $3n_H = \int_0^{\omega_D} g(\omega)d\omega$. Here, $g(\omega)$ is the phonon density of states (DOS), which in the Debye model is given by:

$$g(\omega) = \frac{V_{uc}}{2\pi^2}\frac{\omega^2}{v_s^3} \tag{2}$$

with V_{uc} the unit cell volume.[2]

The Debye temperature can then be deduced as $\hbar\omega_D = k_B\Theta_D = \left(\frac{6n_H\pi^2}{V_{uc}}\right)^{1/3}\hbar v_s$ [44–46], while the isochoric heat capacity in the Debye model is then given as [47]:

$$C_v^D = 9n_H N_A k_B \left(\frac{k_B T}{\hbar\omega_D}\right)^3 \int_0^{\hbar\omega_D/k_B T} \frac{x^4 e^x}{[e^x-1]^2}dx \tag{3}$$

where $x = \frac{\hbar\omega}{k_B T}$, N_A and k_B are the Avogadro number and the Boltzmann constant. The Debye temperatures of type-I clathrates reported in literature obtained from this approach are in the 200–300 K range [31–35,37–39,41,48].

The Einstein-like phonon subsystem in clathrates is usually ascribed to the guest atoms exhibiting large atomic displacement parameters, which are assumed to behave as independent Einstein oscillators ("rattling modes") [32–35,37–39,41]. These oscillators (8 in the case of type-I clathrates) have three degrees of freedom, therefore the number of Einstein modes amounts to $n_E = 24$. These modes, however, are not all equivalent, which is due to the different cage geometries within the unit cell. Assuming three different Einstein temperatures (or energies), the isochoric heat capacity, C_v^E, associated to the Einstein guest subsystem is then expressed as a discrete sum over the contributions of these vibrations, $C_v^E = \sum_{i=1-3} C_v^{E_i}$ with $C_v^{E_i}$ being the isochoric heat capacity of a single Einstein oscillator characterized by its energy E_i (or temperature Θ_i^E):

$$C_v^{E_i} = N_A k_B \left(\frac{E_i}{k_B T}\right)^2 \frac{e^{\frac{E_i}{k_B T}}}{(e^{\frac{E_i}{k_B T}}-1)^2} \tag{4}$$

To resume, in this specific heat model for type-I clathrates, the 3 N (*i.e.* 162 vibrational modes) are shared between a stiff Debye solid counting for 138 modes and a network of independent Einstein oscillators which represents 24 modes. The four microscopic parameters of this model are hence the Debye energy, $\hbar\omega_D$, which can be fixed if the average sound velocity and the three Einstein energies, E_{1-3}.

Fig. 3(a) reports the specific heat divided by T^3 as a function of temperature recorded for the Ge-type I clathrate $Ba_{7.81}Ge_{40.67}Au_{5.33}$ in comparison to fitting results obtained with the here described model. This clearly highlights the excess of specific heat over the T^3 Debye-dependence at low T: a broad peak appears, with its maximum at a low temperature of around 25 K. The observed broad hump above the low temperature Debye part ($\sim T^3$), is a typical finding in type-I clathrates [13,24,49]. It has often been linked to the physics of glasses and rather misleadingly associated to the presence of disorder, mainly related to the rattling motions of the guest atoms in the large cages [33,34,36–39,49,50]. On the other hand, this excess of heat capacity has been reproduced by *ab initio* lattice dynamics calculations using fully ordered structural models with harmonic interactions, thus showing that it is merely the consequence of an increased phonon density of states at low energy [51].

In the applied model of $C_v(T)$, the Debye background originates from the stiff cages and deviations over it are successfully reproduced by the three Einstein peaks characterized by the energies E_{1-3}. In

[2] The elementary volume per phonon is $\frac{(2\pi)^3}{V_{uc}}$. In the Debye model, the volume between two iso-energy surfaces is $4\pi q^2 dq = 4\pi\frac{\omega^2}{v_s^3}d\omega$ (with $\hbar\omega = v_s q$). Thus $\int g(\omega)d\omega = \int \frac{V_{uc}}{2\pi^2}\frac{\omega^2}{v_s^3}d\omega$.

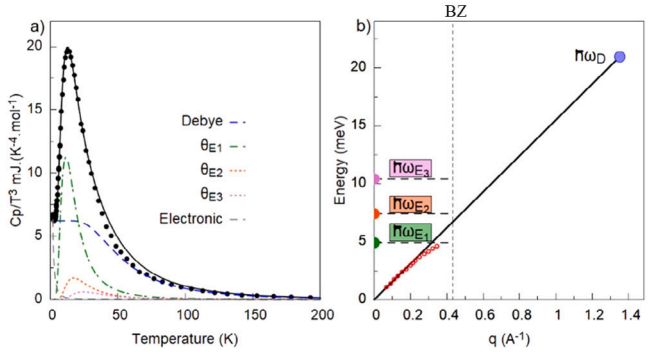

Fig. 3. Specific heat and phonon spectrum interpreted in the classical Debye model. (a) Measured isobaric heat capacity divided by T^3 versus T in the type-I clathrate $Ba_{7.81}Ge_{40.67}Au_{5.33}$ (black solid points) [15,24]. The model fit (black line) is decomposed into its Debye component (dashed blue line) and three Einstein peaks characterized by the temperatures $\theta_{E_{1,2,3}}$. The electronic contribution has been considered in the fit at low temperature (dashed gray line). (b) Corresponding microscopic representation of the phonon spectrum obtained from the parameters extracted from the fit shown in (a). The red points correspond to the measured acoustic dispersion in the first Brillouin zone (BZ). (For interpretation of the references to color in this figure legend, the reader is referred to the web version of this article.)
Source: Adapted from [14,15].

Fig. 3(a), the global fit as well as Debye and Einstein contributions are shown. The Debye component dominates the heat capacity for temperatures above 50 K. The fitting parameters obtained for this model are $\hbar\omega_D$ = 20.9 meV (Θ_D = 243 K), E_1 = 4.9 meV (Θ_{E_1} = 57.4 K), E_2 = 7.4 meV (Θ_{E_2} = 85.4 K) and E_3 = 10.4 meV (Θ_{E_3} = 120.6 K). This is in good agreement with the range of published Debye and Einstein temperatures for type-I clathrates that were extracted in similar ways [33–39,41].

Fig. 3(b) shows the microscopic translation of the parameters extracted from the fit by depicting the corresponding scenario of the phonon spectrum in the energy–momentum phase space (**q**, ω). The straight line starting at the origin represents the acoustic linear dispersion which contains 138 phonon modes that disperse up to the Debye energy $\hbar\omega_D$. In the phase space, the three Einstein modes result in three lines at constant energies E_1, E_2 and E_3. For a direct comparison, the measured acoustic dispersion (red open circles) is also depicted [14,15]. Clearly, the phonon spectrum derived from the applied fitting model is not consistent with what is experimentally observed in clathrates. The experimental data emphasize the fact that acoustic phonons do not propagate up to the Debye energy (21 meV), but that the acoustic regime is instead restricted to a small energy range roughly limited by the energy E_1 (~4–5 meV). Moreover, there are not only three discrete energies corresponding to optical non–dispersive phonon modes, but rather several spectral distributions consisting of a large number of guest and host optical branches, whose energies are distributed from $\hbar\omega_{E1}$ to a cutoff energy of about 25 meV, see Fig. 1(d). Still, the positions of the Einstein modes extracted from the heat capacity model are consistent with the median energies of the optical phonon distributions at low energy reported by spectroscopic measurements and located at energies 5, 7.5, 10 and 12 meV [14,15]. This, on the other hand, is not true for the Debye temperature obtained with this model, which clearly has no meaning at the microscopic level. The formula, $k_B\Theta_D = \left(\frac{6n_H\pi^2}{V_{uc}}\right)^{1/3}\hbar v_s$ with n_H = 46, widely used in the literature [48] to estimate the Debye temperature from the sound velocity is meaningless with respect to a physical interpretation and should be avoided. The Debye background in the heat capacity is significantly overestimated, thus resulting in wrong relative weights of Debye and Einstein components in the heat capacity. As we will see below, the overestimation of the acoustic mode heat capacity results in underestimation of their mean free path when determining the lattice thermal conductivity via kinetic gas theory. The origin of this mistake lies in the fact that the guest atoms should not be viewed as independent and isolated Einstein oscillators and sole contributors to the optical part of the spectrum. Indeed, the guest and the host atoms are coherently coupled and their low energy dynamics in the acoustic regime are completely entangled, see [28].

The capped Debye model: a meaningful microscopic model

In this section, we now derive a simple and meaningful model for the heat capacity on the basis of the Einstein and Debye components in line with the one proposed Agne et al. [52] and formerly introduced by Toberer [8]. Moreover, the free parameters of the model are directly related to the microscopic parameters determined by means of phonon spectroscopy.

The capped acoustic dispersion

For setting up our model in the simplest manner, a single isotropic acoustic branch with a sound velocity, v_s, is assumed, which extends up to the limit of the acoustic regime, *i.e.* up to $\hbar\omega_{op}$ with the associated temperature $k_B\theta_{op} = \hbar\omega_{op}$. The fundamental difference in our model with respect to the classical one described above is thus the fact that **Debye and Einstein contributions are not assigned on the basis of the atomic species but with respect to the nature of the phonon modes**. While in the classical Debye model, the Debye energy is defined by the number of atoms in the host framework (see Eq. (2)), in the here presented model, on the other hand, the total number of Debye modes, named $3n_D$ is determined from the phonon density of states and the energy $\hbar\omega_{op}$ which limits the acoustic range:

$$3n_D = \int_0^{\hbar\omega_{op}} g(\hbar\omega)d\hbar\omega \tag{5}$$

In the case of a linear dispersion, this leads to the following relation between the sound velocity, $\hbar\omega_{op}$ and n_D:

$$n_D = \frac{V_{uc}}{6\pi^2}\left(\frac{\omega_{op}}{v_s}\right)^3 \tag{6}$$

Hence, the acoustic contribution to the isochoric specific heat is completely determined by the microscopic variables, $\hbar\omega_{op}$ (or $k_B\theta_{op}$) and n_D:

$$C_v^{capped}(T) = 9n_D N_A k_B\left(\frac{k_BT}{\hbar\omega_{op}}\right)^3\int_0^{\hbar\omega_{op}/k_BT}\frac{x^4e^x}{[e^x-1]^2}dx \tag{7}$$

As seen from Eq. (6), the number of the Debye modes n_D is a variable determined by ω_{op} and v_s, which should be less or equal 1. The case n_D = 1 corresponds to the integration of an acoustic branch over the whole first Brillouin zone, meaning that the Debye dispersion accounts for a maximum of three modes, the three acoustic modes. n_D = N, on the other hand, would describe the scenario of the classical Debye model in which the Debye branch integrates all 3 N degrees of freedom of the N atom unit cell. Assuming the same sound velocity, the energy range of the Debye regime is thus reduced by a factor $N^{1/3}$ when n_D changes from N to 1. This renormalization of the Debye energy by $N^{1/3}$ was formerly introduced by Roufose and Klemens [53], who assumed that the acoustic phonons, *i.e.* three modes only, dominate the thermal conduction in complex crystalline materials. They argued that the flattening of the optical branches, caused by the structural complexity, drastically lowers the group velocity of optical phonons, thus minimizing their contribution to thermal transport (see also the review by Slack [44]). Unfortunately, this renormalization has been forgotten especially when adapting the classical Debye model for complex systems. However, there is also no reason to fix the value of n_D to 1, particularly in the case of the acoustic dispersion in complex materials. Indeed, experimentally and theoretically, the acoustic dispersion is not linear in the entire Brillouin zone but bends over and flattens when approaching the edge of the optical continuum at $\hbar\omega_{op}$ as it

can be seen in Fig. 1(d). As has been discussed earlier [16,17,27], the acoustic modes progressively loose their acoustic character which is experimentally seen as an abrupt decrease of their spectral weight and theoretically associated to a drastic change of the phonon participation ratio. In type-I clathrates, this has been related to an increase of the guest atom contribution to the acoustic modes [16]. Hence, the case $n_D = 1$ can be understood as the upper bound of the Debye contribution to the heat capacity and therefore can be associated to the lowest value of the phonon mean free path when describing the lattice thermal conductivity in the framework of kinetic gas theory, as will be discussed later.

In the following, we apply these considerations by using the capped Debye model for energies lower than $\hbar\omega_{op}$, while extending it with an Einstein model at higher energies in order to clarify the respective roles of the Debye and Einstein modes in the thermal properties of clathrates.

Einstein-like heat capacitors

For energies higher than $\hbar\omega_{op}$, the phonon spectrum can be viewed as a continuum of Einstein modes as sketched in Fig. 2. This continuum spreads from $\hbar\omega_{op}$ (or $\hbar\omega_D$) to a maximum energy which will be called $\hbar\omega_{max}$ ($k_B\theta_{max} = \hbar\omega_{max}$). As the number of Debye modes is not any more fixed by the number of atoms in the host network, the number of Einstein modes cannot be related to the number of atoms in the guest network either, but becomes a variable: $3n_E$. Still, the number of Debye, $3n_D$, and Einstein, $3n_E$, modes remain related to each other, as their sum must be equal to the total number of modes in the system. Once the average sound velocity and the energy $\hbar\omega_{op}$ are known, it is straightforward to determine these two variables, through the following relations:

$$\begin{cases} 3n_E + 3n_D = 3N \\ n_D = \frac{V_{uc}}{6\pi^2}\left(\frac{\omega_{op}}{v_s}\right)^3 \end{cases} \quad (8)$$

The distribution of phonon modes in the Einstein continuum can be approximated as Dirac comb of equidistant optical phonon branches. The density of states of such Einstein modes is then given as:

$$g_E(\hbar\omega) = \frac{3n_E}{\hbar\omega_{max} - \hbar\omega_{op}} \quad (9)$$

Consequently, the Einstein component of the heat capacity is obtained by an integral over all the Einstein modes in the Dirac comb, with the isochoric heat capacity of a single Einstein mode ($C_v^{E_i}$) given in Eq. (4). With the above introduced density of states the heat capacity of the Einstein continuum can be expressed as:

$$C_v^E(T) = 3n_E N_A k_B \left[\frac{k_B T}{(\hbar\omega_{max} - \hbar\omega_{op})}\int_{\hbar\omega_{op}/k_BT}^{\hbar\omega_{max}/k_BT}\frac{x^2 e^x}{(e^x-1)^2}dx\right] \quad (10)$$

(C_v^E above is in J mol^{-1} K^{-1}). In the high temperature limit, $k_BT \gg \hbar\omega_{max}$ (x→0), the term in brackets equals unity and the heat capacity reaches the Dulong and Petit limit for the corresponding number of Einstein modes: $C_v^E(k_BT \gg \hbar\omega_{max}) = 3n_E N_A k_B$.

Application

The only free parameters of the model are $\hbar\omega_{op}$, $\hbar\omega_{max}$ and the number of Debye (n_D) or Einstein modes (n_E), which are related by Eq. (8). For the case of $Ba_{7.81}Ge_{40.67}Au_{5.33}$, a fit of the heat capacity obtained with this simple model is shown in Fig. 4(a), with the different contributions plotted separately. A fit without any constraints yields θ_{op} = 47.8 K ($\hbar\omega_{op}$ = 4.12 meV), θ_{max} = 316.5 K ($\hbar\omega_{max}$ = 27.3 meV) and n_D = 0.348. This leads to an average sound velocity v_s = 2450 m s^{-1}. In Fig. 4(b), the microscopic representation of the model with these fitting parameters is depicted by intentionally using the same momentum and energy ranges as in Fig. 3(b). The microscopic parameters ($\hbar\omega_{op}$, $\hbar\omega_{max}$ and v_s) obtained from the fit are in a remarkable agreement with the

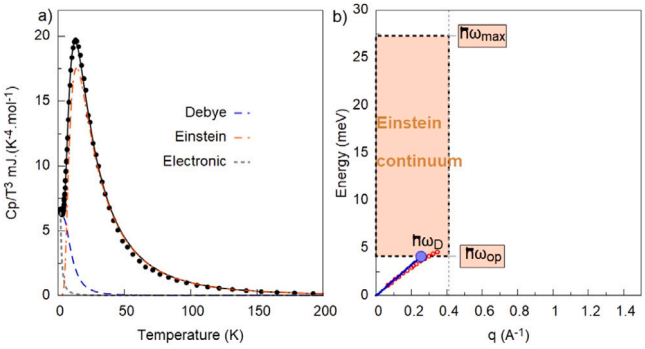

Fig. 4. Heat capacity and phonon spectrum described in the capped Debye model. (a) Measured heat capacity, C_p, divided T^3 versus temperature (T) in $Ba_{7.81}Ge_{40.67}Au_{5.33}$ (black solid points). The fit (black line) is decomposed into its Debye component (dotted blue line) and its Einstein component (solid red line). The electronic contribution has been considered in the fit at low temperature (dotted gray line). (b) Corresponding microscopic representation of the capped Debye model in the energy–momentum space. The TA branch disperses up to the edge of the Einstein continuum, $\hbar\omega_D = \hbar\omega_{op}$. The experimental TA dispersion is superimposed (red circles). The dotted gray lines indicate the borders of the Brillouin zone. (For interpretation of the references to color in this figure legend, the reader is referred to the web version of this article.)

experimental acoustic phonon dispersion also reported in the figure (red open circles). The difference with the classical Debye model is the fact that the discrete number of Einstein modes associated to the dynamics of the guest atoms is replaced by a continuum of modes which dominate the phonon spectrum over a wide energy range, from $\hbar\omega_{op}$ to $\hbar\omega_{max}$. At a macroscopic level, this results in the Einstein contribution determining the heat capacity over a wide temperature range above about ~25 K, as illustrated in Fig. 4(a). In the classical model, on the other hand, it is the Debye contribution which dominates, as shown in Fig. 3(a). Hence, in the capped Debye model, clathrates are mostly *Einstein-like heat capacitors*, which is in clear contrast to results obtained with the standard Debye approach. In fact, the Debye component to the heat capacity is only of importance at low temperature, $T \ll \theta_{op}$, which is consistent with the spectroscopically evidenced confinement of the acoustic phonons in a small energy range [0: $\hbar\omega_{op}$].

In principle, if three acoustic branches are considered, n_D might be expected to be equal to unity. However, here, we actually find $n_D \sim 1/3$ which can be understood as a way to take the branch bending and the loss of the propagative nature of the acoustic phonons into account when approaching $\hbar\omega_{op}$, as mentioned above and also reported in several studies [16,17,22,27]. Indeed, the experimentally observed depletion of the acoustic spectral weight, accompanied by a decrease of the phonon participation ratio, is found for a critical wave-vector well below the border of the first Brillouin zone [16,22]. This critical wave-vector, q_c, can be in principle also extracted from the capped Deby model by defining $q_c = \frac{\hbar\omega_{opt}}{v_s}$. If we consider the dispersion of the transverse acoustic phonon branch propagating along the [110] direction in $Ba_{7.81}Ge_{40.67}Au_{5.33}$, the ratio between q_c and the wave-vector at the zone boundary of the first BZ, q_{BZ}, can then be expressed as:

$$\frac{q_c}{q_{BZ}} = \frac{\hbar\omega_{op}}{v_s}\frac{a}{\sqrt{2}\pi} \quad (11)$$

with a the corresponding lattice parameter. An estimation of this ratio using the experimental values for $Ba_{7.81}Ge_{40.67}Au_{5.33}$for the transverse acoustic branches [14,15], $\hbar\omega_{op}$ ~ 4.5 meV, v_s ~ 3000 m s^{-1}, a = 10.8 Å, yields $\frac{q_c}{q_{BZ}}$ ~0.6. Since the density of states in the Debye model is proportional to the square of the energy and thus the square of the wave-vector, we find that the fraction of propagative acoustic modes, before the propagative character is lost (when the acoustic branch starts to bend) amounts to $\left(\frac{q_c}{q_{BZ}}\right)^2 \sim 0.36$. This is in remarkable

agreement with the value of n_D that is obtained from the fit of the heat capacity with the above described model. Hence, the heat capacity in type-I clathrates is indeed satisfactorily described by three microscopic parameters: v_s, $\hbar\omega_{op}$ (v_s, $\hbar\omega_{op}$ and n_D are linked through the Eq. (6)) and $\hbar\omega_{max}$.

Debye like thermal conductivity and its minimum

As shown in the previous section, the clathrate isochoric specific heat at room temperature is strongly dominated by the Einstein-like contribution. Here, we now formally apply the above introduced simple model description of the specific heat for the determination of the lattice thermal conductivity divided in a Debye and a Einstein part as expressed in Eq. (1). It will be demonstrated that, in contrast to the specific heat, the thermal conductivity is dominated by the acoustic phonons. This leads to the specific situation of *type-I clathrates being Einstein-like heat capacitors but Debye-like thermal conductors.*

Debye-like thermal conductors

As elaborated in the previous sections, the Debye part of the phonon spectrum contains well-defined acoustic phonon modes with energies lower than $\hbar\omega_{op}$. Using the Boltzmann transport equation for phonons, the thermal conductivity associated to this part of the phonon spectrum can then be expressed as:

$$\kappa_D^{capped}(T) = \frac{1}{3}\int_0^{\hbar\omega_{op}} C_v(\hbar\omega,T)v(\hbar\omega)^2\tau(\hbar\omega)g(\hbar\omega)d\hbar\omega \quad (12)$$

The additional microscopic information needed to calculate the thermal conductivity of an acoustic phonon branch is the energy dependence of the phonon lifetime as a function of temperature, $\tau(\hbar\omega,T)$. Unfortunately, it is not easy to experimentally access $\tau(\hbar\omega,T)$, which explains the very few reports that can be found in literature, $Ba_{7.81}Ge_{40.67}Au_{5.33}$ being one of these rare cases [28]. By considering the experimentally determined energy dependence of the relaxation time in $Ba_{7.81}Ge_{40.67}Au_{5.33}$, κ_D^{capped} at 300 K can be estimated, yielding a value of 1.18 W m^{-1} K^{-1}. Since the experimentally determined lattice thermal conductivity amounts to 1.1 W m^{-1} K^{-1}, this result indicates that most of the thermal transport is indeed ensured by acoustic phonons [15].

For a further simplified description of the Debye part of the lattice thermal conductivity, we assume the sound velocity and phonon lifetime to be constant, which transforms Eq. (12) in the following expression:

$$\kappa_D^{capped}(T) = \frac{1}{3}C_v.v_s.\ell \quad (13)$$

where v_s and ℓ are the average sound velocity and phonon mean free path ($\ell = v_s.\tau$). This equation is well known from kinetic gas theory [47,54–56], however, here solely the Debye part of the heat capacity will be considered. At elevated temperature, the Dulong–Petit limit for the isochoric molar heat capacity can be applied, meaning: $C_{v,m}^{D}(300\text{ K}) \approx C_{v,m}^{DP} = 3n_D N_A k_B$ (in J mol^{-1} K^{-1}).

For the classical Debye model, where n_D is assumed to correspond to the number of host atoms ($n_D = n_H = 46$), the Dulong–Petit limit yields $C_{v,m}^{DP} = 3n_D N_A k_B \sim 1753$ kJ m^{-3} K^{-1}. By inserting the experimental lattice thermal conductivity of 1.1 W m^{-1} K^{-1} (at 300 K) and an average sound velocity of 3000 m s^{-1} in Eq. (13), the phonon mean free path can be deduced for this scenario. It amounts to 5–6 Å, which is smaller than the dimensions of the clathrate unit cell (~1 nm). In the past, this small value has been related to the distance between two guest atoms, which were interpreted as scattering centers [31,48]. On the other hand, in the capped Debye model, the number of Debye phonon modes is drastically reduced, resulting in a value of $n_D = 0.35$, as discussed above. Thus $C_{v,m}^{DP}$ amounts to only ~11 kJ m^{-3} K^{-1} for $n_D = 0.35$ and ~32 kJ m^{-3} K^{-1} for $n_D = 1$ and the corresponding phonon mean free path varies in the nanometer range between 30–90 nm. This significantly increased mean free path is in good agreement with experimental findings from neutron scattering [15] and validates the assumption that the thermal conductivity in clathrates is mainly dominated by Debye-like phonons.

In order to understand the key parameters determining the high temperature ("high" relatively to θ_{op}, *i.e.* $T \gg \omega_{op}$) limit of the Debye contribution to the lattice thermal conductivity, we explicitly rewrite Eq. (13), using $n_D = \frac{V_{uc}}{6\pi^2}\frac{\omega_{op}^3}{v_s^3}$ as derived for the capped Debye model (see Eq. (6)). Doing so, κ_L can be expressed as a function of the sound velocity, the DP limit of the isochoric heat capacity, $C_v^{DP} = 3n_D k_B/V_{uc}$, and the low frequency edge of the Einstein continuum, ω_{op}:

$$\kappa_D^{capped}(T \gg \theta_{op}) = \frac{n_D k_B v_s l}{V_{uc}} = \frac{k_B}{6\pi^2}\frac{\omega_{op}^3}{v_s^2}\ell \quad (14)$$

In this formula, the thermal conductivity decreases with the inverse of the square of the sound velocity. While this seems counterintuitive at first glance, microscopically an increase of the sound velocity for a fixed acoustic limit $\hbar\omega_{op}$ actually implies a decrease of the number of available phonon states (or a decrease of the phase space volume for the acoustic branches). Thus, the maximum κ_L is obtained when the number of acoustic states in the interval from 0 to $\hbar\omega_{op}$ reaches its upper limit, *i.e.* for $n_D = 1$, meaning a total of three acoustic modes. The maximum value of the high temperature thermal conductivity, κ_L^{max}, becomes:

$$\kappa_D^{capped,max}(T \gg \theta_{op}) = \frac{k_B}{V_{uc}}v_s\ell \quad (15)$$

Hence, the upper limit of the lattice thermal conductivity at high temperature ($T \gg \omega_{op}$) is determined by the product of the mean free path and the sound velocity. In the case of type-I clathrates, considering $V_{uc} \sim 1$ nm^3 and $v_s \sim 3000$ m s^{-1}, Eq. (15) yields $\kappa_L^{max} = 0.04\ell$ with ℓ in nm. Assuming $\ell \sim 30$ nm as the average of the acoustic phonon mean free path in $Ba_{7.81}Ge_{40.67}Au_{5.33}$ [15], one obtains $\kappa_L^{max} \sim 1.2$ W m^{-1} K^{-1}, very close to the experimental value.

A more accurate expression of the thermal conductivity can be obtained from the frequency integral of κ_D given in Eq. (12), by inserting the high temperature limit of $C_v = 3n_D k_B/V_{uc}$ and assuming the typical quadratic frequency dependence of the phonon lifetime due to Umklapp (U) phonon scattering processes, $\tau(\omega) = a_U\omega^{-2}$. This then cancels out with the frequency dependence of the phonon density of states (see Eq. (2)), thus, after integration, yielding a linear ω_{op} dependence:

$$\kappa_D^{capped,U}(T) = \frac{k_B}{2\pi^2}a_U\frac{\hbar\omega_{op}}{v_s} \quad (16)$$

The prefactor a_U associated to the amplitude of the Umklapp processes is often given as $a_U = \frac{\bar{M}v_s^3}{V_{uc}^{1/3}\gamma T}$ with $\bar{M}$ the average mass and γ the Grüneisen parameter [8]. Considering the latter expression for a_U in Eq. (16) leads to: $\kappa \propto v_s^2\omega_{op}$. This expression is actually close to the phenomenological relation reported by Ikeda et al. [24] for different type-I clathrates, where κ is found to scale with $v_s\omega_{op}$. However, as there are always significant discrepancies among the values of the sound velocity extracted from different techniques, we want to emphasize the consistent main finding that the thermal conductivity scales with the energy $\hbar\omega_{op}$, which determines the size of the energy range available for acoustic phonons. This shows that, despite being confined to a small energy range and largely outnumbered by optical phonons, the acoustic phonons are still the dominant heat carriers in type-I clathrates.

In the light of such findings, it is clear that a strategy for reducing κ_D would imply choosing a heavy guest atom, leading to small values for $\hbar\omega_{op}$ since $\hbar\omega_{op}$ roughly scales with $\frac{1}{\sqrt{M_{Guest}}}$. An alternative and interesting strategy, recently proposed by Viennois et al. [26] is to decrease $\hbar\omega_{op}$ by using other clathrate families with different cage sizes. Looking at the type-IX binary clathrate $Ba_{24}Si_{100}$, these authors have found guest modes with energies as low as 2 meV. For an even further reduction of κ_D, the phonon mean free path could be limited, *e.g.* by

introducing defects or nanostructuring, or eventually exchanging atoms for increasing the sound velocity. Based on the just discussed findings a minimum value of the lattice thermal conductivity is derived in the next section.

Approching the minimum lattice thermal conductivity

In the context of the capped Debye model, a minimum of the lattice thermal conductivity is obtained when the momentum–energy phase space for the acoustic phonons is suppressed (assuming a non-zero lifetime for these modes). In order to estimate the resulting limit, the well-known models for minimum lattice thermal conductivity [44,45,47] have to be adapted to the case of the capped Debye model. Based on the microscopic description of the phonon spectrum discussed above, the minimal thermal conductivity, κ_{min}^{Tot}, can then be assumed to consist of an Einstein, κ_{min}^{E}, and a Debye, κ_{min}^{D}, minimum contribution:

$$\kappa_{min}^{Tot} = \kappa_{min}^{E} + \kappa_{min}^{D} \tag{17}$$

The minimum lattice thermal conductivity: The Debye contribution

Slacks model for the minimum thermal conductivity [44] assumes a minimum mean free path, l^{min}, of half the phonon wavelength, which in case of a linear dispersion relation ($\omega = v_s q$) results in:

$$\ell^{min}(\omega) = \pi \frac{v_s}{\omega} \tag{18}$$

(note here we use the angular frequency $\omega = 2\pi\nu$ while in Slack's paper the frequency ν is used). By displaying the dimensionless fraction $x = \frac{\hbar\omega}{k_B T}$, ℓ^{min} is rewritten as : $\ell^{min} = \pi v_s \frac{\hbar}{k_B T}\frac{1}{x}$.

To get an idea about the order of magnitude of the minimum Debye contribution, phonons within the acoustic regime of $Ba_{7.81}Ge_{40.67}Au_{5.33}$ can be considered. An acoustic mode, at *e.g.* an energy of 3 meV exhibits a group velocity of around 2000 m s^{-1}. This results in $\ell^{min} = 12$ Å, which is in the order of the unit cell dimensions. Experimentally, the mean free path of such phonons was observed to be ~30 nm (at 300 K) [15]. Hence, the situation in $Ba_{7.81}Ge_{40.67}Au_{5.33}$ is still far from the Slack criterion for minimum thermal conductivity.

Assuming an acoustic phonon mean free path corresponding to ℓ_{min} in combination with the heat mode capacity of the capped Debye model which corresponds to the integrand in the integral given in Eq. (7), the minimum thermal conductivity of the Debye part of the spectrum, κ_{min}^{D}, in the context of the kinetic gas theory (see Eq. (13)) reads:

$$\kappa_{min}^{D} = \frac{1}{4\pi} k_B \frac{\omega_{op}^2}{v_s} \left[2\left(\frac{k_B T}{\hbar\omega_{op}}\right)^2 \int_0^{\hbar\omega_{op}/k_B T} \frac{x^3 e^x}{(e^x-1)^2} dx \right] \tag{19}$$

(expressed in W m^{-1} K^{-1}). One can rewrite Eq. (19) as function of $\theta_{op}(= \frac{\hbar\omega_{op}}{k_b})$ and n_D and find the expression derived by Cahill and Pohl [45][3]

In the high temperature limit, defined by $k_B T \gg \hbar\omega_{op}$, the term in brackets goes to one and the minimum thermal conductivity of the Debye contribution becomes:

$$\kappa_{min}^{D}(k_B T \gg \hbar\omega_{op}) \sim \frac{k_B}{4\pi}\frac{\omega_{op}^2}{v_s} \tag{20}$$

[3] Eq. (19) rewritten as function of θ_{op} and n_D reads as Cahill and Pohl's formula reported in [45] (see their formula (19)): $\kappa_{min}^{D} = \left(\frac{9\pi}{16}\right)^{1/3} k_B \left(\frac{n_D}{a^3}\right)^{2/3} v_s \left[2\left(\frac{T}{\theta_{op}}\right)^2 \int_0^{\theta_{op}/T} \frac{x^3 e^x}{(e^x-1)^2} dx\right]$. There is a factor 3 between our constant $1/\left(\frac{9\pi}{16}\right)^{1/3} = 1/0.827$ and their: 1/2.48 which is due to the 3 different polarizations. Deriving their formulas, Cahill and Pohl were considering 1 Debye mode while in our formula in Eq. (19), we have considered the average sound velocity for the three polarization.

leading to a quadratic dependence on the energy $\hbar\omega_{op}$. In the case of $Ba_{7.81}Ge_{40.67}Au_{5.33}$, with the experimental values $\hbar\omega_{op}$ = 4.5 meV and v_s = 3000 m s^{-1} [15], we find $\kappa_{min}^{D}(k_B T \gg \hbar\omega_{op}) \sim 0.02$ W m^{-1} K^{-1}. This value is coherent with the calculations for κ_{min}^{D} calculated by Ikeda et al. [24], by using a similar modified Debye model. Thus, when the acoustic phonon mean free path is reduced at its minimum value, the minimum of the total lattice thermal conductivity is mostly determined by its Einstein part which is roughly one order of magnitude higher. In the SI, we discuss the value of the mean free path of acoustic phonons for which the Debye and Einstein contribution to the thermal transport equalize.

Thermal conductivity of the Einstein-like phonons

For the n_E Einstein like phonon modes spread in an energy range between $\hbar\omega_{op}$ and $\hbar\omega_{max}$, the concept of a random walk of the thermal energy is used to determine the minimum thermal conductivity. Assuming an oscillator i, characterized by its temperature θ_E^i or energy $\hbar\omega_E^i$, the oscillation period is given by:

$$T_E^i = \frac{2\pi}{\omega_E^i} = \frac{2\pi\hbar}{k_B \theta_E^i} \tag{21}$$

After a certain time, τ_E^i, an excited oscillator will release its energy to its nearest neighbors. The oscillation times can be expressed as a multiple of the oscillation period, *i.e.*, $\tau_E^i = \alpha_E^i T_E^i$.

In the limit of strong damping, typically used to describe the thermal transport in disordered materials, the smallest oscillation time is assumed to be half the oscillation period, resulting in $\tau_E = T_E/2$ with $\alpha_E = 1/2$ [45,47]. In the type-I clathrates $Ba_{7.81}Ge_{40.67}Au_{5.33}$, four distributions of optical modes with energies $E_{1,2,3}$ = 4.5, 7, 9.6 and 11.5 meV, have been experimentally observed [14,15]. Among them, only the first one at E_1 can be viewed as a well defined one-phonon peak, showing an oscillation period of $T_{E_1} \sim 0.9$ ps. Hence, the oscillation time of this mode, as derived from its lifetime, ~1.35 ps, corresponds to about 1.5 times its period (*i.e.* $\alpha_E^i = 1.5$). The oscillation periods of the other peaks at $E_{2,3,4}$ are $T_{E_{2,3,4}} \sim 0.6$, 0.43 and 0.36 ps. Since these peaks rather consist of a distribution of optical phonon branches, they cannot be viewed as one-phonon peaks. Thus, the observed lifetimes (0.66, 0.64 and 0.54 ps [15]), can only be transferred in a lower limit for the oscillation time of the optical phonons contained in these peaks, yielding $\tau_{E_2} \geq 1.1 T_{E_2}$, $\tau_{E_{3,4}} \geq 1.5 T_{E_{3,4}}$. The situation in type-I clathrates is thus different from the strong damping limit applied in disordered materials, as the Einstein oscillators store their energies significantly longer than half a oscillation period.

After an average time equal to the oscillation time, the oscillator can release its energy through different channels. The minimum distance that this amount of released energy will travel in the material is basically given by the interatomic distance. Thus, from the oscillation time and the smallest distance between two Einstein oscillators, one can define a velocity for the diffusive energy propagation, called *thermal velocity* [45]. Here, the average interatomic distance can simply be estimated as $\ell = \left(\frac{V_{uc}}{N}\right)^{1/3}$. Note that the notation ℓ – earlier used for the phonon mean free path – is kept as this distance can be understood as a sort of energy mean free path. The thermal velocity is then given by:

$$v_E^i = \frac{\ell}{\alpha_E^i T_E^i} = \frac{1}{\alpha}\frac{1}{\pi}\left(\frac{V_{uc}}{N}\right)^{1/3} \frac{k_B \theta_{E_i}}{\hbar} \tag{22}$$

where the same $\alpha_E^i = \alpha = 1.5$ has been assumed for all modes. The larger α, the smaller is the thermal velocity and thus the thermal conductivity. This is due to the fact that the energy rather than being transferred, is stored in the oscillations of the Einstein phonons (for large α values). In the following, the lower limit of the lattice thermal conductivity of the optical phonons in intermetallic clathrates will be estimated for $\alpha = 1.5$. From Eq. (22), the thermal velocity of the

optical mode at E_1 amounts to about 250 m s^{-1}, which is one order of magnitude smaller than the sound velocity.

Using the above expression of the thermal velocity, the oscillating time and in combining it with the density of states and the mode heat capacity as given in Eq. (4), the thermal conductivity for the continuum of Einstein oscillators, $\kappa^E(T)$ can finally be expressed as:

$$\kappa^E(T) = \frac{n_E k_B}{3\pi\alpha N^{2/3}} \frac{1}{a} \frac{\omega_{op}+\omega_{max}}{2} \left[\frac{2k_B^2 T^2}{\hbar^2\omega_{max}^2 - \hbar^2\omega_{op}^2} \int_{\hbar\omega_{op}/k_BT}^{\hbar\omega_{max}/k_BT} \frac{x^3 e^x}{(e^x-1)^2} dx \right] \quad (23)$$

In the high temperature limit defined by $k_BT \gg \hbar\omega_{max}$ the term in brackets is equal to 1. Moreover, for the case of a unit cell with a large number of atoms, as in the type-I clatrathes, Eq. (23) simplifies due to $n_E \sim N$ (since $n_D \ll n_E$). The high temperature limit of κ^E is thus:

$$\kappa^E(T \gg \theta_{max}) \sim \frac{k_B}{3\pi\alpha} \frac{1}{\ell} \frac{\omega_{op}+\omega_{max}}{2} \quad (24)$$

where $\ell = \frac{a}{N^{1/3}}$ is the interatomic distance defined above and $\frac{\omega_{op}+\omega_{max}}{2}$ can be viewed as the average Einstein energy of the continuum.

At this point, it is interesting to notice that in order to decrease κ^E_{min}, not the lowest lying optical mode but the center of mass of the continuum is the most important parameter. Hence, for the case of type-I clathrates and, more generally, for complex materials $\hbar\omega_{max} \gg \hbar\omega_{op}$, and therefore the expression further simplifies to:

$$\kappa^E(k_BT \gg \hbar\omega_{max}) \sim \frac{k_B}{3\pi\alpha} \frac{1}{\ell} \frac{\omega_{max}}{2} \quad (25)$$

This indeed clearly shows that the key parameters are the maximum energy of the optical phonon spectrum – mainly dominated by vibrations of the host lattice – and the number of oscillations α. The dependence on the α coefficient is also an interesting, pointing out once more that the minimum value of the lattice thermal conductivity is obtained for the longest oscillation times of the optical Einstein phonons, *i.e.* for long storage time before re-emission in the system. However, the interpretation of the measured optical phonon lifetime may have to be reconsidered within the context of newly evolving theories in which the mutual coherence effects are taken into consideration [57–59]. Indeed, the low energy optical spectrum in clathrates contains dense and highly degenerate modes that can mutually interfere, resulting in excitations that are more coherent. Thus, the observed phonon lifetimes might be a result of such a mutual coherence. Eq. (25) furthermore shows that the minimum of the lattice thermal conductivity decreases by increasing the interatomic distance, *i.e.* by lowering the particle density of the material.

In the case of $Ba_{7.81}Ge_{40.67}Au_{5.33}$, with $3n_E = 3 * 56 - 3$, θ_{E1} = 47.8 K and $\hbar\omega_{max}$ = 27.3 meV as found from the fit of the heat capacity, we obtain: $\kappa^E_{min}(T \gg \theta_{max}) \sim 0.11$ W m^{-1} K^{-1} for $\alpha = 1.5$ and 0.16 W m^{-1} K^{-1} for $\alpha = 1$.

Conclusion

Even nowadays, the Deybe model is still widely used to extract microscopic information from specific heat and thermal conductivity measurements. However, typically the origin of this model – simple systems with one atom per (cubic) unit cell – is neglected. This in turn results in applications of the model for situations, which it is not suited for. This becomes particularly problematic when complex crystal structures with many atoms per unit cell and certain particularities in their lattice dynamics are described. Structural complexity, as discussed with respect to intermetallic clathrates, often implies a phonon spectrum that can be divided in two main regimes: the acoustic part, which contains well defined propagative Debye like acoustic modes involving coherent collective motions, and the optical part which contains a broad distribution of dispersion-less Einstein like optical phonons. The low energy edge of the optical continuum, determined by $\hbar\omega_{op}$, defines the transition between the Debye and the Einstein regime. This splitting of the phonon spectrum is the main effect of the structural complexity and is common to any organic or inorganic complex crystals. For such cases, the classical Debye model fails badly. The reason for this failure is the limited energy range for acoustic phonon modes which has to be taken into account. To allow for a proper description of such a scenario, the capped Debye model has been derived by considering only modes below the optic continuum and by, moreover, introducing $3n_D$ (instead of $3N$) as the number of Debye-like phonons (acoustic modes with a dispersive character). This modified Debye is based on a microscopically meaningful picture. In combination with a continuum of Einstein-like optical modes $3(N-n_D)$, it allows for an excellent fitting of the specific heat, furthermore, yielding microscopic parameters that correspond to insights gained from spectroscopic measurements. While this modified description of the specific heat has been applied for the case of clathrates, it is evident that it in principle can be applied to any type of material.

With the modified description of the specific heat it is then also possible to gain insight in the lattice thermal conductivity of type-I clathrates. For the case of $Ba_{7.81}Ge_{40.67}Au_{5.33}$, it was shown that starting from the modified Debye model, a microscopically correct description of the lattice thermal conduction can be achieved. The experimentally observed phonon mean free paths of more than 30 nm can only be reconciled with usually applied models for the lattice thermal conductivity, if a reduction of the acoustic regime and thus a specific heat as described in the capped Debye model is considered. The Einstein part of the phonon spectrum contains the highest number of phonon modes, typically ~3N (as $N \gg n_D$), and therefore dominates the heat capacity. On the other hand, while the number of Debye modes is small, these modes remain propagative with large mean free paths and consequently contribute largely to the lattice thermal conductivity. Thus, as a result of the structural complexity, the phonon states that dominate the lattice thermal conductivity and the heat capacity are different. Hence, these systems can be viewed as Einstein-like heat capacitors and Debye-like thermal conductors.

Finally, it has to be emphasized again that the number of Debye modes is determined by the sound velocity and the energy $\hbar\omega_{op}$, moreover, being limited to a maximum value of $n_D = 1$. Its value is not only determined by the number of atoms in the unit cell but also the chemical composition and the topology of the unit cell. Thus, having an infinite number of atoms in the unit cell ($N \to \infty$) is not enough to minimize the acoustic (or Debye) part of the lattice thermal conductivity. In addition, increasing N adds the number of modes in the optical continuum which consequently rises the optical (or Einstein) contribution to the lattice thermal conductivity. Hence, an efficient way to reduce the Debye contribution to the lattice thermal conductivity is either to reduce the number of Debye modes (which can be achieved by decreasing $\hbar\omega_{op}$) or to decrease the acoustic phonon mean free path. In type-I clathrates, the latter one is still a few orders of magnitude higher than its minimum value, such that nanostructurating the grain size below 100 nm by either sintering bulk powders or the growth of nano-films, or introducing extended defects are possible options for bulk materials. On the other hand, the Einstein contribution to the lattice thermal conductivity can be minimized by lowering the maximum energy $\hbar\omega_{max}$ and by increasing the storage time of the mode energy, *i.e.* the average time after which an excited oscillator releases its energy. Thus, in type-I clathrates, a further reduction of the lattice thermal conductivity to about 0.5 W m^{-1} K^{-1} (at 300 K), going along with an increase in thermoelectric efficiency, seems reasonable.

CRediT authorship contribution statement

S. Pailhès: Project administration, Supervision, Conceptualization, Methodology, Software, Validation, Formal analysis, Writing – original draft, Writing – review & editing. **V.M. Giordano:** Conceptualization, Validation, Funding acquisition, Formal analysis, Writing – review & editing. **S.R. Turner:** Formal analysis, Software, Data curation. **P.-F.**

Lory: Formal analysis, Software, Data curation. **C. Candolfi:** Formal analysis, Writing – review & editing. **M. de Boissieu:** Conceptualization, Validation, Funding acquisition, Formal analysis, Writing – review & editing. **H. Euchner:** Supervision, Conceptualization, Methodology, Software, Validation, Formal analysis, Writing – original draft, Writing – review & editing.

Declaration of competing interest

The authors declare that they have no known competing financial interests or personal relationships that could have appeared to influence the work reported in this paper.

Data availability

Data will be made available on request.

References

[1] Snyder GJ, Toberer ES. Complex thermoelectric materials. Nature Mater 2008;7:105–14.

[2] Klarbring J, Hellman O, Abrikosov IA, Simak SI. Anharmonicity and ultralow thermal conductivity in lead-free halide double perovskites. Phys Rev Lett 2020;125(4):045701. http://dx.doi.org/10.1103/physrevlett.125.045701.

[3] Even J, Paofai S, Bourges P, Letoublon A, Cordier S, Durand O, Katan C. Carrier scattering processes and low energy phonon spectroscopy in hybrid perovskites crystals. In: Freundlich A, Lombez L, Sugiyama M, editors. SPIE proceedings. SPIE; 2016, http://dx.doi.org/10.1117/12.2213623.

[4] Yu Y, Cagnoni M, Cojocaru-Mirédin O, Wuttig M. Chalcogenide thermoelectrics empowered by an unconventional bonding mechanism. Adv Funct Mater 2019;30(8):1904862. http://dx.doi.org/10.1002/adfm.201904862.

[5] Yang H, yue Yang J, Savory CN, Skelton JM, Morgan BJ, Scanlon DO, Walsh A. Highly anisotropic thermal transport in $LiCoO_2$. J Phys Chem Lett 2019;10(18):5552–6. http://dx.doi.org/10.1021/acs.jpclett.9b02073.

[6] Hoang K, Johannes MD. Defect physics in complex energy materials. J Phys: Condens Matter 2018;30(29):293001. http://dx.doi.org/10.1088/1361-648x/aacb05.

[7] Toberer ES, Baranowski LL, Dames C. Advances in thermal conductivity. Annu Rev Mater Res 2012;42(1):179–209. http://dx.doi.org/10.1146/annurev-matsci-070511-155040.

[8] Toberer ES, Zevalkink A, Snyder GJ. Phonon engineering through crystal chemistry. J Mater Chem 2011;21:15843.

[9] Verchère A, Pailhès S, Floch SL, Cottrino S, Debord R, Fantozzi G, Misra S, Candolfi C, Lenoir B, Daniele S, Mishra S. Optimum in the thermoelectric efficiency of nanostructured Nb-doped TiO_2 ceramics: from polarons to Nb-Nb dimers. Phys Chem Chem Phys 2020;22(23):13008–16. http://dx.doi.org/10.1039/d0cp00652a.

[10] Grin Y. Inhomogeneity and anisotropy of chemical bonding and thermoelectric properties of materials. J Solid State Chem 2019;274:329–36. http://dx.doi.org/10.1016/j.jssc.2018.12.055.

[11] Bouyrie Y, Candolfi C, Pailhès S, Koza MM, Malaman B, Dauscher A, Tobola J, Boisron O, Saviot L, Lenoir B. From crystal to glass-like thermal conductivity in crystalline minerals. Phys Chem Chem Phys 2015;17:19751. http://dx.doi.org/10.1039/c5cp02900g.

[12] Rull-Bravo M, Moure A, Fernandez JF, Martin-Gonzalez M. Skutterudites as thermoelectric materials: revisited. RSC Adv 2015;5:41653–67. http://dx.doi.org/10.1039/C5RA03942H.

[13] Takabatake T, Suekuni K, Nakayama T, Kaneshita E. Phonon-glass electron-crystal thermoelectric clathrates: Experiments and theory. Rev Modern Phys 2014;86(2):669–716. http://dx.doi.org/10.1103/RevModPhys.86.669.

[14] Turner SR, Pailhès S, Bourdarot F, Ollivier J, Raymond S, Keller T, Sidis Y, Castellan J-P, Lory P-F, Euchner H, Baitinger M, Grin Y, Schober H, de Boissieu M, Giordano VM. Impact of temperature and mode polarization on the acoustic phonon range in complex crystalline phases: A case study on intermetallic clathrates. Phys Rev Res 2021;3(1):013021. http://dx.doi.org/10.1103/physrevresearch.3.013021.

[15] Lory P-F, Pailhès S, Giordano VM, Euchner H, Nguyen HD, Ramlau R, Borrmann H, Schmidt M, Baitinger M, Ikeda M, Tomes P, Mihalkovic M, Allio C, Johnson MR, Schober H, Sidis Y, Bourdarot F, Regnault LP, Ollivier J, Paschen S, Grin Y, de Boissieu M. Direct measurement of individual phonon lifetimes in the clathrate compound $Ba_{7.81}Ge_{40.67}Au_{5.33}$. Nat Commun 2017. http://dx.doi.org/10.1038/s41467-017-00584-7.

[16] Pailhès S, Euchner H, Giordano VM, Debord R, Assy A, Gomès S, Bosak A, Machon D, Paschen S, de Boissieu M. Localization of propagative phonons in a perfectly crystalline solid. Phys Rev Lett 2014;113:025506.

[17] Euchner H, Pailhès S, Nguyen LTK, Assmus W, Ritter F, Haghighirad A, Grin Y, Paschen S, de Boissieu M. Phononic filter effect of rattling phonons in the thermoelectric clathrate $Ba_8Ge_{40+x}Ni_{6-x}$. Phys Rev B 2012;86:224303.

[18] Koza MM, Johnson MR, Viennois R, Mutka H, Girard L, Ravot D. Breakdown of phonon glass paradigm in La- and Ce-filled Fe_4Sb_{12} skutterudites. Nature Mater 2008;7(10):805–10. http://dx.doi.org/10.1038/nmat2260.

[19] Shibata K, Currat R, de Boissieu M, Sato TJ, Takakura H, Tsai AP. Dynamics of the ZnMgY icosahedral phase. J Phys: Condens Matter 2002;14(8):1847–63. http://dx.doi.org/10.1088/0953-8984/14/8/313.

[20] de Boissieu M, Currat R, Francoual S, Kats E. Sound-mode broadening in quasicrystals: A simple phenomenological model. Phys Rev B 2004;69:054205. http://dx.doi.org/10.1103/PhysRevB.69.054205, URL https://link.aps.org/doi/10.1103/PhysRevB.69.054205.

[21] Norouzzadeh P, Myles CW, Vashaee D. Phonon dynamics in type-VIII silicon clathrates: Beyond the rattler concept. Phys Rev B 2017;95. http://dx.doi.org/10.1103/PhysRevB.95.195206.

[22] Euchner H, Pailhès S, Giordano VM, de Boissieu M. Understanding lattice thermal conductivity in thermoelectric clathrates: A density functional theory study on binary Si-based type-I clathrates. Phys Rev B 2018;97(1). http://dx.doi.org/10.1103/physrevb.97.014304.

[23] Dong J, Sankey OF, Myles CW. Theoretical study of the lattice thermal conductivity in Ge framework semiconductors. Phys Rev Lett 2001;86(11):2361–4. http://dx.doi.org/10.1103/physrevlett.86.2361.

[24] Ikeda MS, Euchner H, Yan X, Tomeš P, Prokofiev A, Prochaska L, Lientschnig G, Svagera R, Hartmann S, Gati E, Lang M, Paschen S. Kondo-like phonon scattering in thermoelectric clathrates. Nature Commun 2019;10(1). http://dx.doi.org/10.1038/s41467-019-08685-1.

[25] Tadano T, Tsuneyuki S. Quartic anharmonicity of rattlers and its effect on lattice thermal conductivity of clathrates from first principles. Phys Rev Lett 2018;120(10). http://dx.doi.org/10.1103/physrevlett.120.105901.

[26] Viennois R, Koza MM, Debord R, Toulemonde P, Mutka H, Pailhès S. Anisotropic low-energy vibrational modes as an effect of cage geometry in the binary barium silicon clathrate $Ba_{24}Si_{100}$. Phys Rev B 2020;101(22):224302. http://dx.doi.org/10.1103/physrevb.101.224302.

[27] Euchner H, Gross A. Predicting accurate phonon spectra: An improved description of lattice dynamics in thermoelectric clathrates based on the SCAN meta-GGA functional. Chem Mater 2019;31(7):2571–6. http://dx.doi.org/10.1021/acs.chemmater.9b00216, arXiv:https://doi.org/10.1021/acs.chemmater.9b00216.

[28] Pailhès S, Giordano VM, Lory P-F, Boissieu MD, Euchner H. Nanostructured semiconductors. CRC Press; 2016, p. 47. http://dx.doi.org/10.1201/9781315364452.

[29] Holland MG. Analysis of lattice thermal conductivity. Phys Rev 1963;132(6):2461–71. http://dx.doi.org/10.1103/physrev.132.2461.

[30] Michael B, Duong NH, Christophe C, Iryna A, Katrin M-K, Igor V, Valeriy R, Mykola H, Raul C-G, Ulrich B, Bodo B, Lukyan A, Yuri G. Thermoelectric characterization of the clathrate-I solid solution $Ba_{8-d}Au_xGe_{46-x}$. Appl Phys Lett 2021;119(6):063902. http://dx.doi.org/10.1063/5.0059166, arXiv:https://doi.org/10.1063/5.0059166.

[31] Christensen M, Johnsen S, Iversen BB. Thermoelectric clathrates of type I. Dalton Trans 2010;39:978–92. http://dx.doi.org/10.1039/b916400f.

[32] Sales BC, Chakoumakos BC, Jin R, Thompson JR, Mandrus D. Structural, magnetic, thermal, and transport properties $X_8Ga_{16}Ge_{30}$ (X = Eu, Sr, Ba) single crystals. Phys Rev B 2001;63(24). http://dx.doi.org/10.1103/physrevb.63.245113.

[33] Xu J, Tang J, Sato K, Tanabe Y, Heguri S, Miyasaka H, Yamashita M, Tanigaki K. Heat capacity study on anharmonicity in $Ae_8Ga_{16}Ge_{30}$ (Ae = Sr and Ba). J Electron Mater 2011;40(5):879–83. http://dx.doi.org/10.1007/s11664-011-1607-z.

[34] Nolas GS, Weakley TJR, Cohn JL, Sharma R. Structural properties and thermal conductivity of crystalline Ge clathrates. Phys Rev B 2000;61:3845. http://dx.doi.org/10.1103/PhysRevB.61.3845.

[35] Umeo K, Avila MA, Sakata T, Suekuni K, Takabatake T. Probing glasslike excitations in single-crystalline $Sr_8Ga_{16}Ge_{30}$ by specific heat and thermal conductivity. J Phys Soc Japan 2005;74(8):2145–8. http://dx.doi.org/10.1143/jpsj.74.2145.

[36] Avila MA, Suekuni K, Umeo K, Fukuoka H, Yamanaka S, Takabatake T. Glasslike versus crystalline thermal conductivity in carrier-tuned $Ba_8Ga_{16}X_{30}$ clathrates (X = Ge, Sn). Phys Rev B 2006;74:125109. http://dx.doi.org/10.1103/PhysRevB.74.125109.

[37] Suekuni K, Avila MA, Umeo K, Takabatake T. Cage-size control of guest vibration and thermal conductivity in $Sr_8Ga_{16}Si_{30-x}Ge_x$. Phys Rev B 2007;75:195210. http://dx.doi.org/10.1103/PhysRevB.75.195210.

[38] Suekuni K, Avila MA, Umeo K, Fukuoka H, Yamanaka S, Nakagawa T, Takabatake T. Simultaneous structure and carrier tuning of dimorphic clathrate $Ba_8Ga_{16}Sn_{30}$. Phys Rev B 2008;77(23). http://dx.doi.org/10.1103/physrevb.77.235119.

[39] Zheng X, Rodriguez SY, Saribaev L, Ross Jr JH. Transport and thermodynamic properties under anharmonic motion in type-I $Ba_8Ga_{16}Sn_{30}$ clathrate. Phys Rev B 2012;85:214304. http://dx.doi.org/10.1103/PhysRevB.85.214304.

[40] Melnychenko-Koblyuk N, Grytsiv A, Fornasari L, Kaldarar H, Michor H, Roehrbacher F, Koza M, Royanian E, Bauer E, Rogl P, Rotter M, Schmid H, Marabelli F, Devishvili A, Doerr M, Giester G. Ternary clathrates BaZnGe: phase equilibria, crystal chemistry and physical properties. J Phys: Condens Matter 2007;19(21):216223. http://dx.doi.org/10.1088/0953-8984/19/21/216223.

[41] Xu J, Wu J, Heguri S, Mu G, Tanabe Y, Tanigaki K. Low-temperature physical properties of $Ba_8Ni_xGe_{46-x}$ (x = 3, 4, 6). J Electron Mater 2012;41(6):1177–80. http://dx.doi.org/10.1007/s11664-011-1898-0.

[42] Leszczynski J, Ros VD, Lenoir B, Dauscher A, Candolfi C, Masschelein P, Hejtmanek J, Kutorasinski K, Tobola J, Smith RI, Stiewe C, Müller E. Electronic band structure, magnetic, transport and thermodynamic properties of in-filled skutterudites $In_xCo_4Sb_{12}$. J Phys D: Appl Phys 2013;46(49):495106. http://dx.doi.org/10.1088/0022-3727/46/49/495106.

[43] Melot BC, Tackett R, O'Brien J, Hector AL, Lawes G, Seshadri R, Ramirez AP. Large low-temperature specific heat in pyrochlore $Bi_2Ti_2O_7$. Phys Rev B 2009;79(22). http://dx.doi.org/10.1103/physrevb.79.224111.

[44] Slack GA. The thermal conductivity of nonmetallic crystals. Solid State Phys 1979;34:1–71. http://dx.doi.org/10.1016/S0081-1947(08)60359-8.

[45] Cahill DG, Pohl RO. Lattice vibrations and heat transport in crystals and glasses. Ann Rev Phys Chern 1988;39:93–121.

[46] Morelli DT, Slack GA. High lattice thermal conductivity solids. In: High thermal conductivity materials. New York, NY: Springer; 2006, p. 37–68. http://dx.doi.org/10.1007/0-387-25100-6.

[47] Kaviany M. Heat transfer physics. Cambridge University Press; 2008.

[48] Christensen M, Abrahamsen AB, Christensen NB, Juranyi F, Andersen NH, Lefmann K, Andreasson J, Bahl CRH, Iversen BB. Avoided crossing of rattler modes in thermoelectric materials. Nat Mater 2008;7:811–5. http://dx.doi.org/10.1038/nmat2273.

[49] Baggioli M, Cui B, Zaccone A. Theory of the phonon spectrum in host-guest crystalline solids with avoided crossing. Phys. Rev. B 2019;100(22):220201. http://dx.doi.org/10.1103/PhysRevB.100.220201.

[50] Liu Y, Xi Q, Zhou J, Nakayama T, Li B. Phonon-glass dynamics in thermoelectric clathrates. Phys Rev B 2016;93(21). http://dx.doi.org/10.1103/physrevb.93.214305.

[51] Christensen S, Schmokel MS, Borup KA, Madsen GKH, McIntyre GJ, Capelli SC, Christensen M, Iversen BB. Glass-like thermal conductivity gradually induced in thermoelectric $Sr_8Ga_{16}Ge_{30}$ clathrate by off-centered guest atoms. J Appl Phys 2016;119:185102. http://dx.doi.org/10.1063/1.4948334.

[52] Agne MT, Hanus R, Snyder GJ. Minimum thermal conductivity in the context of diffuson-mediated thermal transport. Energy Environ Sci 2018;11(3):609–16. http://dx.doi.org/10.1039/c7ee03256k.

[53] Roufosse M, Klemens PG. Thermal conductivity of complex dielectric crystals. Phys Rev B 1973;7(12):5379–86. http://dx.doi.org/10.1103/physrevb.7.5379.

[54] Tritt TM, editor. Thermal conductivity. Physics of solids and liquids, Springer US; 2004, http://dx.doi.org/10.1007/b136496.

[55] Klemens PG. Thermal conductivity and lattice vibrational modes. Solid State Phys 1958;7:1–98.

[56] Carruthers P. Theory of thermal conductivity of solids at low temperatures. Rev Modern Phys 1961;33(1):92–138.

[57] Zhang Z, Guo Y, Bescond M, Chen J, Nomura M, Volz S. Heat conduction theory including phonon coherence. Phys Rev Lett 2022;128:015901. http://dx.doi.org/10.1103/PhysRevLett.128.015901, URL https://link.aps.org/doi/10.1103/PhysRevLett.128.015901.

[58] Simoncelli M, Marzari N. Unified theory of thermal transport in crystals and glasses. Nat Phys 2019;15:809. http://dx.doi.org/10.1038/s41567-019-0520-x.

[59] Isaeva L, Barbalinardo G, Donadio D, Baroni S. Modeling heat transport in crystals and glasses from a unified lattice-dynamical approach. Nature Commun 2019;10:3853. http://dx.doi.org/10.1038/s41467-019-11572-4.